Oxygen 1s ELNES study of perovskites $(Ca,Sr,Ba)TiO_3$

Ziyu Wu[a,b*], F. Langenhorst[c], F. Seifert[c], E. Paris[d] and A. Marcelli[b]

[a] *Beijing Synchrotron Radiation Facility, Institute of High Energy Physics, Chinese Academy of Sciences, P.O. Box 918, Beijing 100039, P.R. China*
[b] *INFN-Laboratori Nazionali di Frascati, P.O.Box 13, I-00044 Frascati, Italy*
[c] *Bayerisches Geoinstitut, Universitat Bayreuth, D-95440 Bayreuth, Germany*
[d] *Dipartimento di Scienze della Terra and INFM, Universita' di Camerino, I-62032 Camerino MC, Italy*

The O K-edge spectra of perovskites $XTiO_3$ with X=Ca, Sr and Ba have been measured using electron energy-loss spectroscopy (EELS) and are analyzed using the *ab initio* full multiple-scattering (MS) calculations. The near-edge structures arise mainly from covalency by direct and/or indirect interaction between oxygen and metal. The coordination number of the cation and the site symmetry also influence the spectral shape and structures. Comparison of full MS simulations of different clusters around the excited atom allows to interpret and correlate the features present in the spectra of each compound to its specific atomic arrangement and electronic structure.

Keywords: XANES, Oxygen K edge, Perovskites

1. Introduction

There is a covalent bonding between oxygen and cations in perovskites (Groot et al.1989; Soriano et al. 1993; Wu et al. 1998). The O 2p orbitals thus have an empty antibonding part due to hybridization with these empty atomic orbitals.This mechanism can be investigated by O K-edge XANES (X-ray absorption near-edge structure) and/or ELNES (electron energy loss near-edge structure) experiments, as it involves, according to the dipole selection rule, a 1s - 2p electronic transition. Moreover, the shape of the O K-edge spectra have been shown to be particularly sensitive to the nature of the transition metal contained (Groot et al. 1989; Aken et al. 1998). So far, XANES has mostly been used to elucidate the electronic and atomic structure of transition metals by measuring their L-edges (Garvie & Craven 1994; Garvie & Buseck 1998; Aken et al. 1998) mostly in fairly simple structures. For the oxygen K-edge spectra, which are of interest here, many technical difficulties associated mainly with the low energy involved (ca. 530 eV) limited the investigation of systems of geological and geochemical interest. For these reasons, the experimental and theoretical analysis of the O K-edges in complex materials is a delicate matter and still very scarce.

Many technical problems associated with the acquisition of O K-edge spectra have been overcomed by the development of high resolution and high throughput monochromators for low energies as well as refinement of the ELNES method (Egerton 1996) which is particularly suited for this energy range. In this paper we present a series of ELNES spectra at the O K edge in perovskites $XTiO_3$ with X = Ca, Sr and Ba. This suite of samples allows us to probe the oxygen-metal bond (where the metal is mostly titanium) and to investigate how the bond is affected by the first and second neighbors, and by the variable coordination geometry. In the light of full MS calculations, we connect the specific atomic arrangement and the electronic structure of each compound to the position, shape and intensity of the characteristic features of the ELNES spectra.

2.Calculations

Calculations were based on the one-electron full multiple-scattering (MS) theory (Stohr 1988; Durham 1988; Lee & Pendry 1975; Natoli 1986) using ``the extended CONTINUUM" code developed by Natoli et al. (Natoli 1980). We have used the Mattheiss prescription (Mattheiss 1964) to construct the cluster electronic density and the Coulomb part of the potential by superposition of neutral atomic charge densities obtained from the Clementi-Roetti tables (Clementi & Roetti 1974). In order to simulate the charge relaxation around the core hole in the photoabsorber of atomic number Z, we have used the screened Z+1 approximation (final state rule) (Lee & Beni 1977), which takes the orbitals of the Z+1 atom and constructs the final state charge density by using the excited configuration of the photoabsorber with the core electron promoted to a valence orbital.

Practical considerations suggest to use a complex-X_α potential as the exchange-correlation part of the potential, i.e. X_α potential (real part) and imaginary part of energy- and position-dependent complex Hedin-Lundquist (H-L) self energy $\Sigma(\mathbf{r}, E)$ (Penn 1987). The later gives the amplitude attenuation of the excited photoelectronic wave due to extrinsic inelastic losses, and takes automatically into account the photoelectron mean free path in the excited final state. The calculated spectra are further convoluted with a Lorentzian function with a full width Γ_h to account for the core hole lifetime (≈0.2eV) and Γ_{exp}, the experimental resolution (≈0.8 eV).

3. Experimental methods

O K-edge ELNES spectra were collected with a Gatan PEELS 666 parallel electron spectrometer attached to a PHILIPS CM20-FEG (field emission gun) TEM operating at 200 kV. The energy resolution of the Schottky field-emitter defined as full width at half maximum height of the zero-loss peak was 0.75 to 0.8 eV. All spectra were collected in diffraction mode with illumination a = 8.0 mrad and collection semiangles b = 1.45 mrad, and a 2 mm PEELS aperture. The measurements of O K-edge spectra were performed with an energy dispersion of 0.1 eV/channel and an integration time t = 10 - 20 s per read-out. Data reduction of these spectra included the correction for dark current and channel-to-channel gain variation, the subtraction of an inverse power law background, and the removal of plural scattering contributions by the Fourier-ratio deconvolution technique. The energy scale of EELS spectra was calibrated by measuring simultaneously the C K-edge of the amorphous carbon foil and the Ti L- and O K-edges of samples with an energy dispersion of 0.3 eV/channel. The π^* peak of the C K-edge at 285 eV served as fix point for the calibration. This procedure makes sure that the energy scales of O K-edge spectra for the different samples are not shifted relative to each other. The spectra of the different samples are therefore directly comparable. Absolute energy values may carry a small systematic error because of uncertainties in the energy dispersion of the spectrometer, estimated to be less than 0.5 eV.

4.Results and discussion

Figure 1 shows the experimental O K-edge ELNES spectra of perovskites $XTiO_3$ with X=(Ca, Sr, and Ba). The spectra are in good agreement with published works (Aken et al.1998; Brydson et al. 1992; Groot et al. 1993). In Fig. 1, one should note the similarity between the $XTiO_3$ spectra but also the distinct differences.

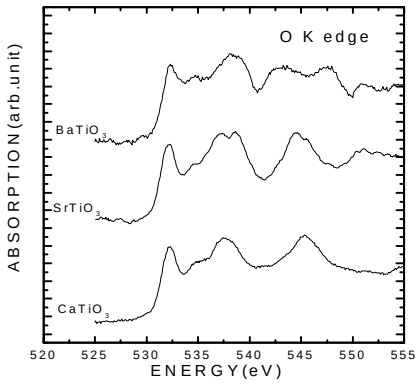

Figure 1
Experimental ELNES spectra at the O K edge for perovskites $XTiO_3$ with X=(Ca, Sr, and Ba).

In the spectra of these three perovskites $XTiO_3$, (X=Ca, Sr, and Ba), a variation in the chemical shift of the first peak is not observed which is different from the Soriano et al.'s results for d^0 oxides of the group IVa and Va elements (Soriano et al. 1993), because the states in the unoccupied bands just above the Fermi level have most weight on the Ti sites in these perovskites. However, a variation in the chemical shift of the first peakis not observed in Nakai's work for alkaline-earth oxides (Nakai et al. 1987).

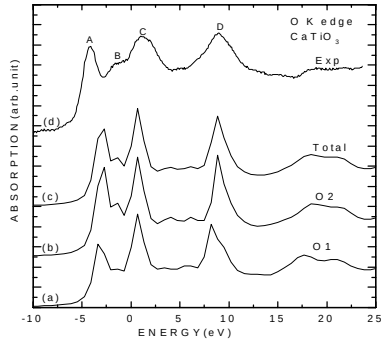

Figure 2
MS calculations at the O K edge for two individual oxygen sites (a and b) and their summation in 1:2 proportion (c) in $CaTiO_3$ using the eight-shell cluster, along with the experimental spectrum (d).

The mineral perovskite $CaTiO_3$ is one of the few minerals having the distorted perovskite structure consisting of slightly deformed TiO_6 octahedra which are rotated relative to their positions in the ideal cubic phase. It has an orthorhombic cell with space group Pbnm (Buttner & Maslen 1992; Beran et al. 1996). In Figure 2 we report two individual oxygen site calculations and their combination in 1:2 proportion (curve (c)), along with experimental data (d). Reasonable good agreement has been achieved and all experimental features A-D are well reproduced. However, the energy separation between features A and C is slightly smaller than the experimental value.

Similar results for $SrTiO_3$ and $BaTiO_3$ are presented in Fig. 3 and Fig. 4, respectively. These perovskites have cubic symmetry ($SrTiO_3$, Pm-3m, with undistorted and unrotated TiO_6 octahedron) or tetragonal symmetry ($BaTiO_3$, P4mm), respectively.

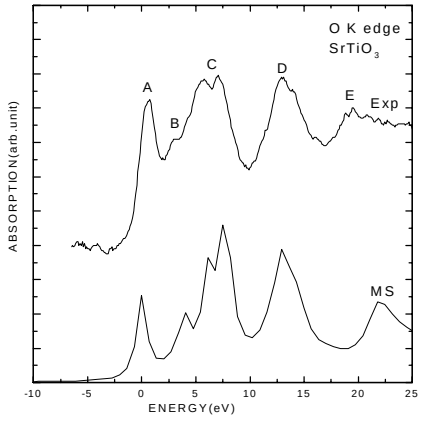

Figure 3
MS calculations at the O K edge in perovskite $SrTiO_3$ using the eight-shell cluster (a), along with the experimental spectrum (b).

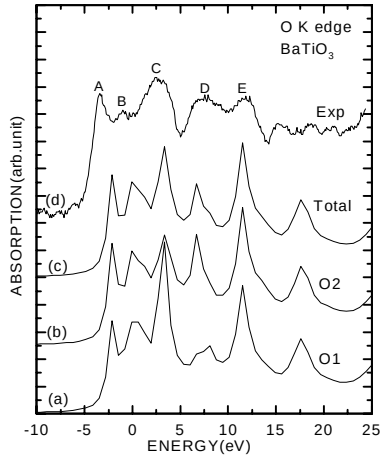

Figure 4
MS calculations at the O K edge for two individual oxygen sites (a and b) and their summation in 1:2 proportion (c) in perovskite $BaTiO_3$ using the eight-shell cluster, along with the experimental spectrum (d).

Structural data have been taken from single crystal X-ray refinement (Hutton & Nelmes 1981; Harada et al. 1970). These results are in disagreement with those obtained by de Groot et al. (Groot et al. 1993). In fact, they have studied the O 1s x-ray absorption spectra of $SrTiO_3$ by using the localized spherical wave method with an extended basis set to describe the unoccupied states over a wider energy range. In their study the calculated density of states for $SrTiO_3$ is in disagreement with the experiment not only for the preedge region but also for the higher energy part. They attributed this disagreement to the core-hole potential, but we cannot exclude the possibility that it is rather due to a wrong Wyckoff position for both oxygen and strontium (see Table I in Groot et al. 1993). From our decomposed MS calculation for $BaTiO_3$ (see Fig.5) taking the O2-site cluster, we find that all prepeaks have disappeared when we suppress the d orbitals of the nearest Ti and Ba atoms (curve (a)). When suppressing the Ba d orbitals only, the preedge peak A remains, indicating that it is mainly due to the Ti d contribution

(curve (b)). Peak B is superimposition by Ti and Ba and C mainly originates from Ba d bands (curves (c) and (d)). This finding is consistent with the band-structure calculation (Groot et al. 1993).

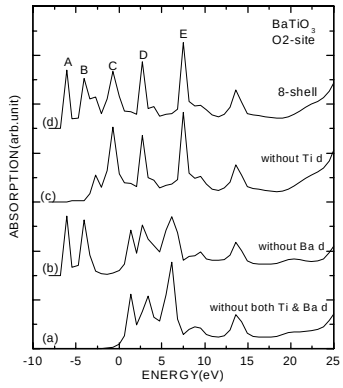

Figure 5
MS calculations of the oxygen K-edge spectra in $BaTiO_3$: (a) the decomposed calculation of the eight-shell cluster taking O2 as the center but suppressing the d bases of Ti and Ba; (b) the same as (a) but suppressing only the Ba d contribution; (c) the same as (a) but suppressing only the Ti d contribution; (d) the normal eight-shell cluster results (without convolution).

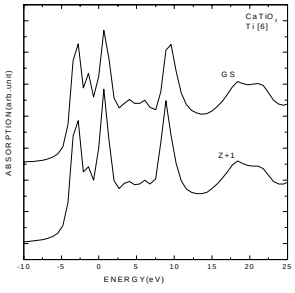

Figure 6
Comparison between two MS calculations at the O K edge for perovskite $CaTiO_3$, using two different final-state potentials: the Z+1 final-state potential (lower curve) and the ground-state (GS) potential (upper curve).

We present in Fig.6 a comparison between the fully relaxed final state (Z+1 approximation) and the ground-state (GS) potential calculations for $CaTiO_3$. The results are quite similar for the two different potential calculations, except for the small difference in the relative intensities. This is because the core hole is now located on the oxygen while the states in the unoccupied bands just above the Fermi level have most weight on the cation site, indicating that the spectrum is rather insensitive to core-hole potential effects, in contrast to the conclusion drawn by de Groot et al. (Groot et al. 1993).

5.Conclusion

We have carried out a detailed experimental and theoretical investigation of O K-edge ELNES spectra for perovskites $XTiO_3$ with X=(Ca, Sr, and Ba). Good agreement between experimental data and MS calculations is achieved. Moreover we demonstrated that MS decomposed analysis offers the possibility, at least in these systems, to extract individual atomic as well as electronic structures in terms of particular bands. The features observed in the first several eV above the edge onset represent a fingerprint of the electronic structure of the cation in the local crystal field. They are also related to the lowest-energy states in the unoccupied conduction band. The alkaline-earth elements (Ca, Sr and Ba) play an important role and a strongly related peak sets in at about 8 eV in these spectra.

The features above 539 eV can be identified by the decomposed MS analysis. They essentially reflect the medium-range order. The spectral behaviours between 541 to 550 eV are quite different due to the different site symmetry.

Acknowledgments

Many thanks to Bayerisches Geoinstitut (Bayreuth,Germany) where this work get started, partially supported by the EC ``Human Capital and Mobility - Access to Large Scale Facilities" programme (Contract No. ERBCHGECT940053 to D.C. Rubie).

References

Aken,P.A. van, Liebscher,B. & Styrsa, V.J. (1998), Phys. Chem. Minerals 25, 323-327; 25, 494; Aken et al. (1999), Phys. Rev. B 60, 3815.

Beran,A. Libowitzky, E. & Armbruster, T. (1996), Canadian Mineral.34, 803-809.

Brydson, R. Sauer, H. & Engel, W. (1992) in Transmission Electron Energy Loss Spectroscopy in Materials Science, eds M.M. Disko, C.C. Ahn and B. Fultz (TMS) p.131-154.

Buttner, R.H. & Maslen, E.N. (1992), Acta Cryst. B 48, 644-649.

Clementi, E. & Roetti, C. (1974), Atomic Data and Nuclear Data Tables, Vol. 14.

Durham, P.J. (1998), in X-ray Absorption: Principles, Applications, Techniques of EXAFS, SEXAFS, XANES, edited by R. Prinz and D. Koningsberger (Wiley, New York).

Egerton, R.F. (1996), Electron Energy-Loss Spectroscopy in the Electron Microscopy, (Plenum Press) 485 pp.

Garvie, L.A.J. & Craven, A.L. (1994), Phys. Chem. Minerals 21} 191-206.

Garvie, L.A.J. & Buseck, P.R. (1998), Nature 396, 667-670.

De Groot, F.M.F, Grioni, M., Fuggle, J.C., Ghijsen, J. Sawatzky, G.A. & Petersen, H. (1989), Phys. Rev. B 40, 5715.

De Groot, F.M.F. et al. (1993), Phys. Rev. B 48, 2074-2080.

Harada, J.Pedersen, T. & Barnea, Z. (1970), Acta Cryst.26} 336-344.

Hutton, J. & Nelmes, R.J. (1981), Acta Cryst. A 37, 916-920.

Lee,P.A. & Pendry, J.B. (1975), Phys. Rev. B 11, 2795.

Lee, P.A. & Beni, G. (1977), Phys. Rev. B 15, 2862.

Mattheiss, L. (1964), Phys. Rev. A 134, 970.

Nakai, S. et al. (1987), Phys. Rev. B 36, 9241-9246.

Natoli, C.R., Misemer, D.K., Doniach, S. & Kutzler, F.W. (1980), Phys. Rev. A 22, 1104.

Natoli, C.R. & Benfatto, M. (1986), J. Phys. (Paris) Colloq. 47, C8-11.

Penn, D.R. (1987), Phys. Rev> B 35, 482.

Soriano, L. Et al. (1993), Solid State Commun. 87, 699.

Stohr, J. (1988), in X-Ray Absorption: Principles, Applications, Techniques of EXAFS, SEXAFS, edited by R. Prinz and D. Koningsberger (Wiley, New York).

Wu, Z.Y., Jollet, F. & Seifert, F. (1998), J. Phys.: Condens. Matter 10, 8083-8092.